

Quantum size effects in Pb/Si(111) investigated by laser-induced photoemission

P. S. Kirchmann,^{1,*} M. Wolf,¹ J. H. Dil,² K. Horn,² and U. Bovensiepen¹

¹*Fachbereich Physik, Freie Universität Berlin, Arnimalle 14, D-14195 Berlin-Dahlem, Germany*

²*Fritz-Haber-Institut der Max-Planck-Gesellschaft, Faradayweg 4-6, D-14195 Berlin-Dahlem, Germany*

(Received 7 December 2006; published 6 August 2007)

We use laser-induced photoemission spectroscopy at 6 eV photon energy to investigate quantum well states of epitaxial Pb films on Si(111) as function of film thickness. The binding energies of the quantum well states were found in good agreement with density-functional calculations for a freestanding Pb slab. An oscillation of the work function with a period of 2 ML was observed as a function of film thickness, which correlates well with the oscillatory electron density at the Fermi level determined from the photoemission spectra.

DOI: [10.1103/PhysRevB.76.075406](https://doi.org/10.1103/PhysRevB.76.075406)

PACS number(s): 73.21.Fg, 79.60.-i, 79.60.Dp

I. INTRODUCTION

Quantum size effects (QSEs) in ultrathin metal films are both of fundamental importance as a probe of basic quantum mechanics¹ and for application as tailored nanostructures.² The pronounced difference of physical properties compared to bulk materials is explained by the formation of discrete quantum well states (QWSs) due to spatial electron confinement in the metal film.^{1,3} When ultrathin metal films approach a thickness comparable to the electron de Broglie wavelength, the system can be considered as a quantum well and a quantization of the electronic band structure perpendicular to the surface may be observed. The electron confinement in the metal film results in several quantum well subbands confined in the metal film, whereas the electronic structure parallel to the surface may be altered, for example, through the interaction with substrate bands,⁴ but remains continuous as a function of parallel momentum $p_{\parallel} = \hbar k_{\parallel}$.

The system Pb/Si(111) has been studied intensively by scanning tunneling microscopy,⁵ photoemission spectroscopy,⁶ (PES) and density-functional theory⁷ (DFT), since it exhibits a rich variety of pronounced QSE. Among these are the preference of “magic” island heights⁸ due to electronically assisted growth, also observed in the formation of the “devil-staircase” phases,⁹ oscillations of the transition temperature of the superconducting state¹⁰ as well as oscillations in the direction, and magnitude of the Hall effect.¹¹ All these properties sensitively depend on the film thickness such that a change of coverage by 1 ML translates into variations of these quantities. The reported oscillation period of 2 ML can be directly linked to the modulation of the electron density at the Fermi level due to the quantization of the $6p_z$ Pb bulk bands. In this respect, the system of Pb/Si(111) may be regarded as a prototype for the observation of such QSE.

An oscillatory behavior of the work function as a function of film thickness in ultrathin metal films has also long been predicted by calculations employing a jellium model¹² and was experimentally confirmed for the case of Ag/Fe(100).¹³ Qualitatively, the surface dipole is modulated due to a change of the electron spillout of the highest occupied QWS wave function. For Pb/Si(111), the work function oscillation was theoretically reinvestigated recently in a DFT calculation of a freestanding Pb slab.⁷

In this paper, we report on discrete QWS in epitaxial Pb films grown as wedges¹⁴ on Si(111) which were investigated

by laser-induced PES employing ultraviolet photons at energies of 6.0 and 5.3 eV. These photon energies are advantageous for the case of metallic QWS on semiconductor substrates because not only sharp QWS peaks are observed but also the sensitivity to Si states is enhanced. The binding energies of the QWS over a wide range of coverage were determined by PES and found to be in good agreement with DFT calculations.⁷ Moreover, a pronounced oscillation of the global sample work function as a function of film thickness was resolved, which is directly correlated to the modulation of the electron density at the Fermi level. The use of Pb wedges enabled us to follow the work function modulation as the coverage is tuned quasicontinuously, as will be shown in the following.

Compared to synchrotron or He-lamp light sources, laser based photoemission at 6 eV photon energy offers several advantages for the study of QSE. Besides the fact that a laser source can be implemented as a tabletop experiment, it also combines a high photon flux with an increased bulk sensitivity¹⁵ due to the rather long mean free path of low-energy electrons in solids.¹⁶ Laser based light sources can also be used for PES with ultrahigh resolution in the submeV range,¹⁷ which permit precise investigations of phenomena such as the gap in the superconducting state and other effects of electron correlation. In addition, time-resolved PES can be carried out by using femtosecond laser pulses.¹⁸ This brings novel insights into the energy relaxation dynamics of occupied electronic states and their coupling to other quasiparticles such as phonons and magnons.¹⁹

II. EXPERIMENT

The PES experiments were carried out in an ultrahigh-vacuum chamber with a base pressure $< 1 \times 10^{-10}$ mbar combined with an amplified, tunable femtosecond laser system.²⁰ The epitaxial Pb films grown as wedges¹⁴ were prepared on a Si(111) surface. The substrate surface was prepared by the standard procedure of repeatedly flashing the sample to 1470 K by resistive heating, followed by cooling at a rate of -1 K/s to 970 K. The cleanliness and macroscopic homogeneity of the Si(111)- 7×7 surface reconstruction were confirmed by low-energy electron diffraction (LEED). Pb was evaporated at a pressure of $\leq 5 \times 10^{-10}$ mbar from a homebuilt water-cooled Knudsen cell. The

evaporation rate was monitored by a quartz microbalance and additionally cross-checked after deposition by comparison of the observed QWS binding energies with DFT calculations. First, the Si(111)-($\sqrt{3} \times \sqrt{3}$)-R30°-Pb reconstruction was prepared by deposition of ~ 3 ML Pb at a rate of 0.5–1.2 ML/min at 100 K substrate temperature. This was followed by annealing the sample to 600 K desorbing the excess Pb, which was performed in front of a LEED optics to directly observe the formation of the ($\sqrt{3} \times \sqrt{3}$)-R30° reconstruction. On this wetting layer, wedges of Pb were grown at 100 K substrate temperature using a sharp-edged tantalum shutter to block part of the evaporation cone while moving the sample at a speed of 0.3 mm/min into the evaporation region.¹⁴ This resulted in Pb wedges with slopes of 1.5–4.0 ML/mm. The sample temperature was kept at 100 K during the whole experiment to suppress surface diffusion of Pb and prevent the formation of Pb islands due to a rupture of films with a metastable thickness.²¹

For laser based PES, photons with $h\nu=6.0$ eV are generated by frequency quadrupling the output of a mode-locked amplified Ti:sapphire laser system at 300 kHz repetition rate.¹⁹ Laser pulses at 5.3 eV photon energy were produced by frequency doubling the output of an optical-parametrical amplifier driven by the regenerative amplifier. The spot size of the incident laser beam at the position of the sample was checked by measurement of the laser power transmitted through a pinhole and confirmed to be $\leq 150 \mu\text{m}$. The photoelectron yield was detected in normal emission by a time-of-flight (TOF) electron spectrometer with an acceptance angle of $\pm 3.5^\circ$ and an energy resolution of ≤ 10 meV at 1 eV kinetic electron energy.²⁰ From the kinetic energy E_{kin} , the binding energy referenced to the Fermi level $E-E_F = E_{kin} + \Phi - h\nu$ was calculated. For the photoemission measurements, the work function of sample and spectrometer were matched using a small bias voltage of ~ 300 mV. The global work function $\Phi = h\nu - E_C$ is precisely determined from the low-energy cutoff E_C of the photoelectron spectra.

III. RESULTS AND DISCUSSION

In Fig. 1, photoemission spectra of a Pb wedge with a slope of 4.0 ML/mm are displayed as spectra from 9 to 26 ML coverage (lower panel) which were taken with a lateral resolution of $100 \mu\text{m}$ by moving the sample in front of the TOF spectrometer. The upper panel shows a color-coded representation of the photoemission intensity. The data exhibit a series of QWS dispersing with coverage, where particularly sharp states are observed in the energy range of the indirect band gap of the Si substrate as indicated by the upper valence-band edge²² (VBE) at $E-E_F = -0.35$ eV. These QWSs are *energetically* located in the indirect Si band gap and are thus *spatially* confined to the Pb film as the wave function of the QWS cannot penetrate into the substrate. At energies $E-E_F < -0.35$ eV, much broader quantum well resonances are observed which are degenerate with occupied Si bands. These states are more prominently seen in Fig. 3 discussed further below. The theoretical results for the QWS binding energies from a DFT calculation of Wei and Chou⁷ for a freestanding Pb film of variable thickness are displayed

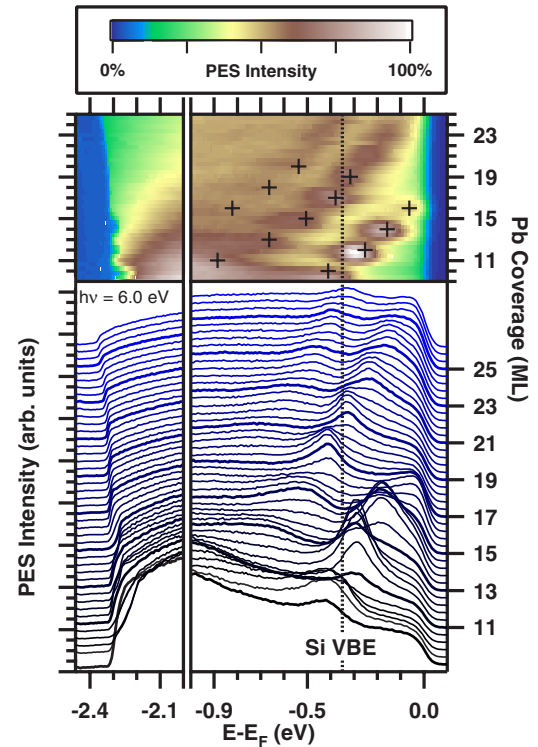


FIG. 1. (Color online) Photoemission spectra of Pb/Si(111) for various coverages observed on a Pb wedge of 4.0 ML/mm slope using 6.0 eV photon energy. The right panel shows a series of discrete QWS dispersing with Pb coverage. The silicon valence-band edge (VBE) is indicated. The upper panel displays the identical data in a false-color representation. The QWS binding energies (+) from a DFT calculation (Ref. 7) are included. In the left panel, the modulation of the low-energy cutoff is highlighted which is a direct measure of the global work function of the Pb film.

as crosses in the color-coded plot of the photoemission yield. Clearly, the DFT data agree well for all three branches of occupied QWS observed experimentally.

The left panel of Fig. 1 focuses on the low-energy cutoff of the photoemission spectra which is a direct measure of the global sample work function. In PES, the global work function—rather than the local one—is accessible due to the macroscopic spot size of the incident light. Contributions from different patches of the surface are averaged which results in a finite width of the low-energy cutoff. Nevertheless, below a coverage of 16 ML, a modulation of work function is clearly observed that vanishes above 16 ML.

In order to perform a proper analysis of the data, it is necessary to take the finite laser spot size into account. On a wedge with a slope of 4.0 ML/mm as in Fig. 1, the laser spot size of $150 \mu\text{m}$ averages over a coverage distribution of 0.6 ML nominal width. The observation of pronounced peaks and work function modulations at low coverage is not hindered by the averaging process which is evident from the contrast of the PES intensity at subsequent monolayers. The intensity of the QWS peaks exhibits a pronounced oscillation with film thickness: For an even film thickness of 10 ML, a high photoemission intensity is observed below the Fermi level, which is significantly reduced at 11 ML and reappears at 12 ML coverage. As the coverage increases to more than

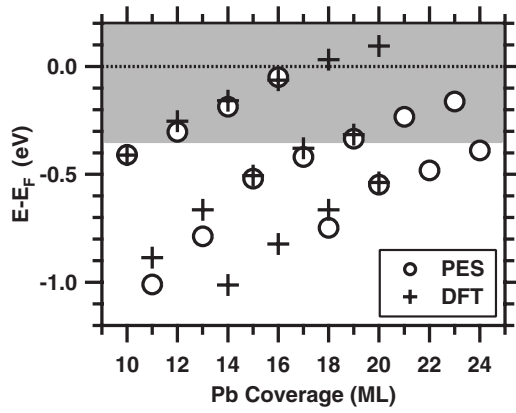


FIG. 2. QWS binding energies as function of coverage as observed by PES and calculated by DFT (Ref. 7). The experimental QWS binding energies were determined from the peak maxima in the photoemission spectra and the error is given by the size of the symbols (\circ). The gray shaded area indicates the fundamental Si band gap.

20 ML, the averaging within the laser spot size reduces the contrast of the discrete QWS and the peaks merge into a continuous branch of QWS. The absence of the work-function modulation for a coverage exceeding 16 ML is explained by neighboring patches of ± 1 ML in the laser spot which give an averaged contribution and broaden the secondary edge. The decrease of the work function by 110 meV for >16 ML and the broadening of the QWS peaks point to a roughening of the Pb films at these coverages.

In Fig. 2, the binding energies determined from the peak maxima in the photoemission spectra are compared to the DFT calculation from Ref. 7 and are generally in good agreement. Some deviations, especially of the quantum well resonances, which are not confined by the Si band gap, might be attributed to the influence of the Si interface. In a phase-accumulation model,¹ electrons of the Pb film are confined by the vacuum barrier and the barrier due to the energy gap of the substrate, such that reflection at the interfaces results in two energy-dependent phase shifts ϕ_{vac} and ϕ_{Si} . These phase shifts have to fulfill the Bohr-Sommerfeld quantization rule:

$$2\pi n = 2\Theta k(E)d + \phi_{vac}(E) + \phi_{Si}(E), \quad (1)$$

with the wave vector k for energy E in the quantized bulk band, the number of monolayers Θ , the interlayer spacing $d=2.86$ Å, and a quantum number n . The presence of the Si interface results in an additional phase shift of the QWS wave function due to a finite penetration of the wave function into the substrate which in turn alters their eigenenergies. As a result, the QWS binding energies observed in very thin films (<10 ML) tend to be larger than predicted by vacuum slab models as the penetration of the wave function into the substrate effectively generates a wider quantum well. Especially, the quantum well resonances at $E-E_F < -0.35$ eV experience this effective widening of the potential well, which results in a significant increase of the binding energy compared to a freestanding Pb slab.

Turning to the QWS confined in the narrow energy region of the Si band gap $E-E_F > -0.35$ eV, one notices that discrete states are observed in the uppermost branch only at coverages of 10, 12, 14, and 16 ML, and in the lower branch at 17, 19, 21, and 23 ML, respectively. This special feature of the Pb/Si(111) QWS is explained by the influence of the Fermi wave vector k_F along the Γ -L direction, where the quantization occurs. The periodicity of QWS crossing the Fermi level is calculated from Eq. (1) to be $\Delta\Theta = \pi/(k_F d)$, where $k_F \approx k$. For a Fermi wave vector²³ $k_F=0.611$ Å⁻¹, this relation yields a period of $\Delta\Theta=1.8$ ML. This means that initially a QWS is expected to cross the Fermi level at every 2 ML because only discrete, integer numbers of monolayers are possible. The small difference between 1.8 and 2.0 ML generates a “beating” effect such that at 5×1.8 ML=9.0 ML, the highest occupied QWS is expected at *odd* and not at *even* coverage and vice versa. Exactly, this odd-even switching behavior is found here as the highest occupied QWSs are observed at even coverage from 10 to 16 ML, each separated by 2 ML. For a coverage >17 ML, the highest occupied QWS can only be supported in a Pb film with odd number of monolayers which is manifested by the series of QWS from 17 to 23 ML. In this context, it is interesting to note an angle-resolved PES study of uniform Pb films on Si(111),²⁴ where this odd-even switching is reported for 13 and 22 ML film thicknesses. However, our results, which show an odd-even switching at a film thickness of 16 ML, are in excellent agreement with the theoretical work of Ref. 7 where a switching is predicted for 7 and 16 ML as well as with previous results from photoemission.²⁵ The occurrence of QWS occupation with a period of 1.8 ML provides a natural explanation for the specific stability of even and odd numbered film thicknesses, on account of the principle of total-energy minimization.²⁶

For a more quantitative analysis of the thickness-dependent work function changes, we have prepared wedges with a reduced thickness gradient and thus increased the coverage resolution. This approach reduces the problem of averaging over different thicknesses by the finite laser spot size. The PES data taken on such a shallow wedge of 1.50 ML/mm slope are shown in Fig. 3 as spectra (bottom) and color-coded intensity plot (top). The decreased slope enhances the thickness resolution to 0.15 ML per spectrum and the QWSs at even film thicknesses of 10, 12, and 14 ML are well separated. The high contrast of the QWS obtained is remarkable: For even thickness, intense and sharp QWSs are observed in the region of the Si band gap, which completely vanish at odd coverage, leaving only a continuous background from elastically and inelastically scattered electrons. The pronounced Fermi edge observed for all film thicknesses indicates the metallic character of the surface and the presence of an intact Pb film. This proves that indeed the averaging due to the finite laser spot size of the scanned region can be neglected. For such a sample, a pronounced work function oscillation is observed in the low-energy cutoff in Fig. 3 which is followed over the entire wedge.

The work function as function of film thickness obtained from the spectra shown in Figs. 1 and 3 is plotted in the lower panel of Fig. 4 in comparison with the theoretical values of Ref. 7. Not only is the periodicity of the experimen-

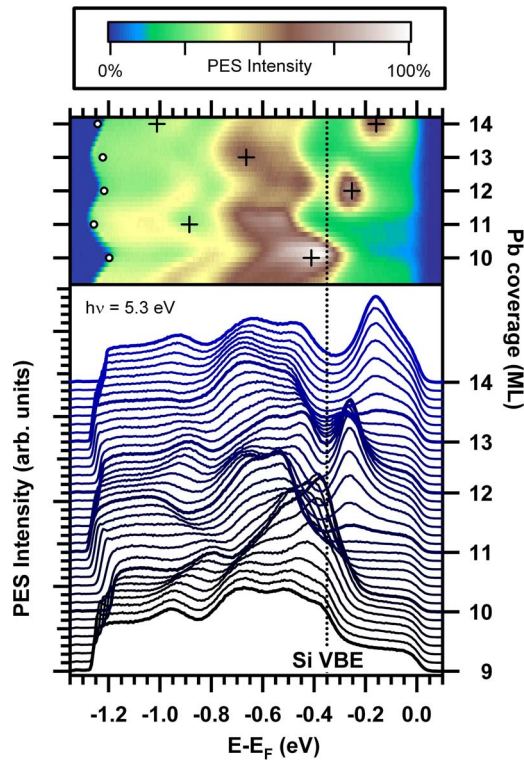


FIG. 3. (Color online) Photoemission spectra of Pb/Si(111) measured at 5.3 eV photon energy on a wedge with 1.5 ML/mm slope. The Si valence-band edge (VBE), the QWS binding energies (+), and work function modulation (O) calculated by DFT (Ref. 7) are indicated.

tally determined oscillations in good agreement with the DFT calculation but also the amplitude of the modulation matches fairly well with the calculated data. The work function oscillations are further analyzed by fitting a phenomenological function⁷ $\Phi(\Theta)$ to the data:

$$\Phi(\Theta) = \frac{A|\sin(k_F d\Theta + \phi_0)| + B}{\Theta^\alpha} + C, \quad (2)$$

where A , B , C , α , and ϕ_0 are constants. The coverage Θ is in this description a continuous variable as used in jellium models.¹² For fixed interlayer spacing d , the fit yields the Fermi wave vector k_F which results in the period of the work function modulation.

The results of the fit of the PES and DFT data are displayed in Fig. 4 as solid and dashed lines, respectively. At first sight, a continuous change of the work function as in a jellium model might appear counterintuitive because the coverage increases locally in integer steps of 1 ML. Our observation is explained by the layer-by-layer growth of the films and the finite resolution of the laser spot. As the coverage Θ is increased on a submonolayer scale, a fraction $0 \leq x \leq 1$ of the probed region has a higher thickness which exhibits a different work function. These different surface patches are averaged within the laser spot. For example, a $\Theta + x$ ML film consists of fraction $1 - x$ patches with Θ ML and x patches

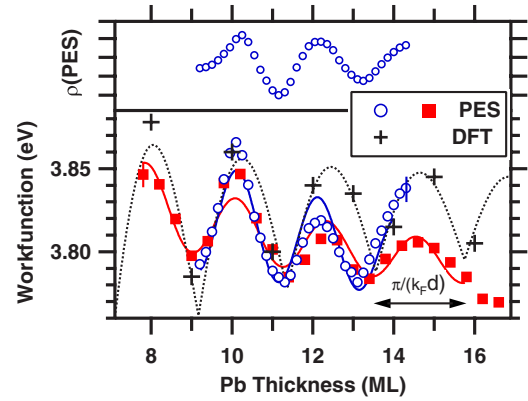


FIG. 4. (Color online) Work function oscillations as a function of film thickness observed in the Pb wedges on Si(111) deduced from the photoemission spectra of Fig. 1 (■) and Fig. 3 (O). The measured data were offset by +186 meV (■) and -183 meV (O) in order to match the theoretical prediction from DFT (Ref. 7). The solid and dashed lines are fits of Eq. (2) to the data points convoluted with a Gaussian function taking into account the finite laser spot size. The upper panel shows the PES intensity $\rho(\text{PES})$ integrated over the region ($E - E_F > -0.35$ eV) of the Si band gap.

with $\Theta + 1$ ML thickness. The work function of a $\Theta + x$ ML film therefore is the weighted arithmetic average of the work functions of a Θ and $\Theta + 1$ ML film.

Fitting a convolution of Eq. (2) and a Gaussian instrument function for 7.8–15.8 ML and 9.2–14.0 ML results in periods of 2.2(1) and 2.0(1) ML for the steep and shallow wedges, respectively. These periods suggest that the work function modulation is directly linked to the periodic modulation of density of states at the Fermi level by the highest occupied quantum well state. The comparison of the position of the maxima of the work function with the appearance of the highest occupied QWS reveals that a confined QWS close to the Fermi level coincides with a maximum of the work function. This is corroborated by a qualitative model of the electron spillout of the QWS wave function at the Pb-vacuum interface.²⁷ A QWS close to E_F will have a significant electron spillout into the vacuum which increases the surface dipole and thereby creates a large work function. The opposite situation of a QWS far from E_F generates a small electron spillout with a small surface dipole and a small work function. This interpretation of the work function in terms of electron density at E_F is supported by the electron density analyzed by PES. In the upper panel of Fig. 4, the photoemission yield $\rho(\text{PES})$ integrated in the region of the Si band gap ($E - E_F > -0.35$ eV) is shown as function of coverage for the shallow wedge. A maximum (minimum) of the electron density appears, which corresponds exactly to the maximum (minimum) of the work function measured for the more shallow wedge (O). The amplitude of this modulation is observed in the electron density and can be linked directly to the magnitude of the work function oscillation.

The increased bulk sensitivity due to the low kinetic energy (< 1 eV) of the photoelectrons generated by the laser allows the observation of electronic states of the Si substrate. Clearly, additional peaks below the Si VBE are observed in Fig. 3. The states oscillating between binding energies of E

$-E_F = -0.9$ and -0.6 eV cannot be assigned to any QWS because the binding energy of these states is modulated and these features are observed at all film thicknesses. Furthermore, they exhibit no intensity modulation as function of film thickness.

IV. CONCLUSION AND OUTLOOK

In summary, we have investigated quantum size effects in Pb/Si(111) by laser based photoemission at UV photon energies of 5–6 eV. The observed QWS binding energies and the modulation of the global sample work-function are found in excellent agreement with recent results from a DFT calculation⁷ of a freestanding Pb film. The work-function oscillation predicted for a quantum well system, which is highly decoupled from the substrate, was resolved with high accuracy. The analysis of the photoemission spectra as function of coverage confirms that the work function modulation is governed by the modulation of electron density below E_F and the electron spillout of the QWS wave function into the vacuum. Additionally, the low kinetic energy of the photoemitted electrons permitted the detection of electronic states

of the Si substrate. These states exhibit a modulation of the binding energy which is correlated to the oscillation of the electron density at the Fermi level induced by the QWS.

Our work highlights the large capabilities of laser based PES with the advantages of high photon flux at small spot sizes in conjunction with increased bulk sensitivity. Furthermore, the use of ultrashort laser pulses adds femtosecond time resolution to the experimentally accessible dependencies. Our future investigations will utilize femtosecond time-resolved two-photon photoemission to further the understanding of energy relaxation dynamics of electrons photoexcited into *unoccupied* QWS. The well understood electronic structure which is readily controlled by variation of the film thickness makes Pb/Si(111) an ideal candidate for the investigation of electron dynamics at the crossover from two and three dimensions.

ACKNOWLEDGMENTS

This work has been funded by the Deutsche Forschungsgemeinschaft through BO 1823/2. P.S.K. and J.H.D. gratefully acknowledge support by the International Max-Planck Research School “Complex Surfaces in Material Science.”

*Electronic address: kirchman@physik.fu-berlin.de; URL: <http://www.physik.fu-berlin.de/~femtoweb>

¹T.-C. Chiang, Surf. Sci. Rep. **39**, 181 (2000).

²J. Barth, G. Costantini, and K. Kern, Nature (London) **437**, 671 (2005).

³M. Milun, P. Pervan, and D. Woodruff, Rep. Prog. Phys. **65**, 99 (2002).

⁴L. Aballe, C. Rogero, P. Kratzer, S. Gokhale, and K. Horn, Phys. Rev. Lett. **87**, 156801 (2001).

⁵R. Otero, A. L. Vazquez de Parga, and R. Miranda, Phys. Rev. B **66**, 115401 (2002).

⁶M. H. Upton, C. M. Wei, M. Y. Chou, T. Miller, and T.-C. Chiang, Phys. Rev. Lett. **93**, 026802 (2004).

⁷C. M. Wei and M. Y. Chou, Phys. Rev. B **66**, 233408 (2002).

⁸Z. Zhang, Q. Niu, and C.-K. Shih, Phys. Rev. Lett. **80**, 5381 (1998).

⁹M. Hupalo, J. Schmalian, and M. C. Tringides, Phys. Rev. Lett. **90**, 216106 (2003).

¹⁰Y. Guo, Y.-F. Zhang, X.-Y. Bao, T.-Z. Han, Z. Tang, L.-X. Zhang, W.-G. Zhu, E. G. Wang, Q. Niu, Z. Q. Qiu, J. F. Jia, Z. X. Zhao, and Q. K. Xue, Science **306**, 1915 (2004).

¹¹I. Vilfan, M. Henzler, O. Pfennigstorf, and H. Pfnür, Phys. Rev. B **66**, 241306(R) (2002).

¹²F. Schulte, Surf. Sci. **55**, 427 (1976).

¹³J. J. Paggel, C. M. Wei, M. Y. Chou, D.-A. Luh, T. Miller, and T.-C. Chiang, Phys. Rev. B **66**, 233403 (2002).

¹⁴R. K. Kawakami, E. Rotenberg, H. J. Choi, E. J. Escorcia-Aparicio, M. O. Bowen, J. H. Wolfe, E. Arenholz, Z. D. Zhang, N. V. Smith, and Z. Q. Qiu, Nature (London) **398**, 132 (1999).

¹⁵J. D. Koralek, J. F. Douglas, N. C. Plumb, Z. Sun, A. V. Fedorov, M. M. Murnane, H. C. Kapteyn, S. T. Cundiff, Y. Aiura, K. Oka, H. Eisaki, and D. S. Dessau, Phys. Rev. Lett. **96**, 017005 (2006).

¹⁶M. Seah and W. Dench, Surf. Interface Anal. **1**, 2 (1979).

¹⁷T. Kiss, F. Kanetaka, T. Yokoya, T. Shimojima, K. Kanai, S. Shin, Y. Onuki, T. Togashi, C. Zhang, C. T. Chen, and S. Watanabe, Phys. Rev. Lett. **94**, 057001 (2005).

¹⁸L. Perfetti, P. A. Loukakos, M. Lisowski, U. Bovensiepen, H. Berger, S. Biermann, P. S. Cornaglia, A. Georges, and M. Wolf, Phys. Rev. Lett. **97**, 067402 (2006).

¹⁹M. Lisowski, P. A. Loukakos, A. Melnikov, I. Radu, L. Ungureanu, M. Wolf, and U. Bovensiepen, Phys. Rev. Lett. **95**, 137402 (2005).

²⁰M. Lisowski, P. A. Loukakos, U. Bovensiepen, J. Stähler, C. Gahl, and M. Wolf, Appl. Phys. A: Mater. Sci. Process. **78**, 165 (2004).

²¹M. Hupalo, S. Kremmer, V. Yeh, L. Berbil-Bautista, E. Abram, and M. C. Tringides, Surf. Sci. **493**, 526 (2001).

²²J. H. Dil, J. W. Kim, T. Kampen, K. Horn, and A. R. H. F. Ettema, Phys. Rev. B **73**, 161308(R) (2006).

²³J. R. Anderson and A. V. Gold, Phys. Rev. **139**, A1459 (1965).

²⁴Y.-F. Zhang, J.-F. Jia, T.-Z. Han, Z. Tang, Q.-T. Shen, Y. Guo, Z. Q. Qiu, and Q.-K. Xue, Phys. Rev. Lett. **95**, 096802 (2005).

²⁵J. H. Dil, J. W. Kim, S. Gokhale, M. Tallarida, and K. Horn, Phys. Rev. B **70**, 045405 (2004).

²⁶D.-A. Luh, T. Miller, J. J. Paggel, M. Chou, and T.-C. Chiang, Science **292**, 1131 (2001).

²⁷N. D. Lang and W. Kohn, Phys. Rev. B **1**, 4555 (1970).